

## AMBIENT TEMPERATURE EFFECT ON SILICON PHOTOVOLTAICS UNDER SIMULATED ENVIRONMENTS

Turkistani Abdulaziz<sup>a</sup>, Kah-Yoong Chan<sup>a\*</sup>, Gregory Soon How Thien<sup>a</sup>, Chun-Lim Siow<sup>b</sup>, Boon Kar Yap<sup>c,d,e</sup>, Ab Rahman Marlinda<sup>f</sup>

<sup>a</sup>Centre for Advanced Devices and Systems, Faculty of Engineering, Multimedia University, 63100 Cyberjaya, Selangor, Malaysia

<sup>b</sup>Centre for Electric Energy and Automation, Faculty of Engineering, Multimedia University, 63100 Cyberjaya, Selangor, Malaysia

<sup>c</sup>Electronic and Communications Department, College of Engineering, Universiti Tenaga Nasional, 43000 Kajang, Selangor, Malaysia

<sup>d</sup>Institute of Sustainable Energy, Universiti Tenaga Nasional, 43000 Kajang, Selangor, Malaysia

<sup>e</sup>International School of Advanced Materials, South China University of Technology, 381 Wushan Road, Tianhe District, Guangzhou, Guangdong, PR China

<sup>f</sup>Nanotechnology and Catalysis Research Centre (NANOCAT), Universiti Malaya, 50603, Kuala Lumpur, Malaysia

### Article history

Received

16 March 2023

Received in revised form

3 May 2023

Accepted

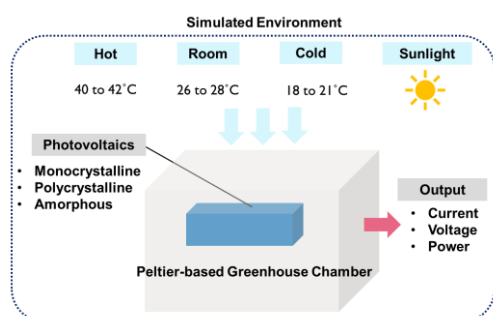
10 July 2023

Published Online

20 October 2023

\*Corresponding author  
kychan@mmu.edu.my

### Graphical abstract



### Abstract

Solar energy is a significant renewable source for home and commercial applications. These solar technologies behave differently depending on the ambient temperature surrounding the devices. Thus, the varying ambient temperature necessitates research into the efficacy of various solar technologies under real-life circumstances. In this study, three types of solar technology were studied, which were polycrystalline, monocrystalline, and amorphous silicon photovoltaics (PVs). All the PVs were tested under various simulated environments (hot, room, and cold temperatures). Additionally, real environmental condition tests under direct sunlight successfully depicted the relationship between solar irradiance and ambient temperature on the PVs. Overall, monocrystalline PV outperformed polycrystalline PV, whereas amorphous PV performed poorly. This observation was evident in the lowest performance reduction of monocrystalline PV in hot (power,  $P_{pv} = 37\%$ ), room ( $P_{pv} = 82\%$ ), cold ( $P_{pv} = 95\%$ ), and direct sunlight ( $P_{pv} = 72\%$ ) conditions. Hence, this research could address the importance of selecting PVs in real-life environments in producing efficient solar PV technologies.

Keywords: Solar energy, monocrystalline silicon, polycrystalline silicon, amorphous silicon, ambient temperature, photovoltaics

### Abstrak

Tenaga suria ialah sumber boleh diperbaharui yang penting untuk aplikasi rumah dan komersil. Teknologi suria ini berkelakuan berlainan bergantung pada suhu ambien yang mengelilingi peranti. Oleh itu, suhu persekitaran yang berbeza memerlukan penyelidikan tentang keberkesanan pelbagai teknologi

suria dalam keadaan sebenar. Dalam kajian ini, tiga jenis teknologi suria telah dikaji, iaitu fotovoltai (PV) silikon polikristal, monokristal, dan amorfus. Semua PV telah diuji di bawah pelbagai persekitaran simulasi (suhu panas, bilik, dan sejuk). Selain itu, ujian keadaan persekitaran sebenar di bawah cahaya matahari berjaya menggambarkan hubungan antara sinaran suria dan suhu ambien pada PV. Secara keseluruhannya, PV monokristal adalah lebih baik berbanding PV polikristal, manakala PV amorfus berprestasi buruk. Pemerhatian ini terbukti dalam pengurangan prestasi rendah PV monokristal dalam keadaan suhu panas (kuasa,  $P_{pv} = 37\%$ ), bilik (kuasa,  $P_{pv} = 82\%$ ), sejuk (kuasa,  $P_{pv} = 95\%$ ), dan bawah cahaya matahari (kuasa,  $P_{pv} = 72\%$ ). Oleh itu, kepentingan PV dalam persekitaran kehidupan sebenar boleh ditangani dalam menghasilkan teknologi PV solar yang cekap melalui penyelidikan ini.

**Kata kunci:** Tenaga suria, monokristal silikon, polikristal silikon, amorfus silikon, suhu ambien, fotovoltai

© 2023 Penerbit UTM Press. All rights reserved

## 1.0 INTRODUCTION

Over the years, the interest in solar panels for converting light to electrical energy has surged [1, 2]. In the current development of solar panels, the design of photovoltaics (PVs) is categorised into several types, such as monocrystalline silicon [3, 4], polycrystalline silicon [5, 6], amorphous thin-film silicon [7], dye-sensitised [8, 9], thin film [2, 10, 11], and perovskite solar cells [12]. In 1941, Ohl *et al.* described silicon cells, which were structured using melt-grown junctions [13]. The related devices demonstrated a power conversion efficiency (PCE) value as low as 1%. Nonetheless, the rapid evolution of PVs depicted massive improvements, in which multi-crystalline cells were utilised to produce PCE values as high as 25% [10]. Hence, the successful discovery of PCE enhancement was owed to the different structures and textures of the fabricated cells.

One of the most reliable and popular types of PVs in current technology was demonstrated by the crystalline silicon PV cells. Concerning the PV structure, crystalline silicon PV cells were produced by selecting one of two boron-doped *p*-type silicon substrates. Therefore, the doping process resulted in the fabrication of monocrystalline and polycrystalline PVs. Monocrystalline PVs were typically fabricated using pseudo-square silicon wafer substrates cut from column ingots grown through the Czochralski process [14]. Alternatively, the polycrystalline PVs differed in their source, which they were fabricated through grown ingots in quartz crucibles. In terms of the typical sizes for both monocrystalline and polycrystalline PVs, their sizes were approximately 5 and 6 inches, respectively.

Thin-film solar cells were another type of PV widely applied in solar energy harvesting technology. The thin-film devices were configured in one of two structures known as substrate or superstrate [15]. The substrate configuration described the structures as metallic coatings on glass or polymer substrates that behaved as the contact. Meanwhile, the superstrate configuration revealed transparent substrates and a

conducting oxide coating on the substrates fabricated the connection. Furthermore, both different structures behaved differently in various weather conditions.

An in-depth study entailing various solar classifications based on fabrication materials revealed that every class from a specific material generated different efficiency percentages [16]. Thus, these findings motivated the objectives of this study in testing several PVs and their corresponding electrical characteristics. Multiple literature studies utilised different methodologies and setups for prototype studies. For example, incandescent, halogen, and low-consuming fluorescent lamps were used to simulate the luminance of sunlight in providing a full spectrum [17]. On the contrary, the light source's colour temperature must be considered when providing the sunlight simulation. For instance, 4800 to 5000 K provided the most precise colour temperature closer to the direct sun. The 5000 to 6800 K range also represented the change in daylight colours [18].

Based on a PV study, both hot and cold weather conditions affected the voltage ( $V_{pv}$ ) and current ( $I_{pv}$ ) values [19]. Generally, these values depicted decreasing behaviours in both situations. Moreover, the  $I_{pv}$  value was higher in summer than in winter. In another study, single-crystal PVs were fabricated and successfully assessed outdoors in Brunei [17]. The variable bipolar operational power supply was tested to measure the panels short-circuit current ( $I_{sc}$ ) and open-circuit voltage ( $V_{oc}$ ). Nonetheless, the study concluded that the monocrystalline PVs' PCE was higher at colder temperatures. In addition, the PCE values decreased once the operating temperature increased.

According to another study, solar irradiance and temperature were highlighted to affect the performance of the amorphous and polycrystalline panels [18]. Therefore, the degradation of these devices was explained in terms of the behaviour of the PVs. One of the main considerations of this study was to investigate the characteristic of PV

technologies. In Malaysia, studies were performed to test various PV performances [19]. A characteristic curve was obtained, which led to an increase until a turning point before decreasing. The justification for this behaviour was mostly related to the influence of solar irradiance and temperature.

Another study in Algeria evaluated the performance of the monocrystalline solar module under different weather conditions, which demonstrated the impact of solar irradiance on the performance curve [20]. The performance curve illustrated that the performance reduced during the irradiance peak. Furthermore, the results indicated that the performance dropped during higher temperatures, which depended on the irradiance and the temperature. From the literature studies mentioned above, solar irradiation and ambient temperature were determined to be the most critical factors that could affect the PVs' performance [21, 22]. A study by Adeb et al. investigated the necessity of environmental temperature optimisation in PVs [23]. The study concluded that ambient temperature influenced annual energy yield in various PVs, rendering it important for large-scale projects. In addition, high temperatures can increase the lattice parameter due to thermal expansion. Thus, this study aimed to determine the extent to which normal daily temperature fluctuations affected the crystal structure of solar panels, focusing on monocrystalline structures.

This study aimed to explore the performance effects of severe ambient temperatures on monocrystalline, polycrystalline, and amorphous PVs. The correct PV selection was necessary to deliver an optimised setting for efficient PVs. Moreover, the study assessed the influence of charge carrier trapping under constant illumination and varied temperatures and the performance of PVs in real-world situations with direct sunshine. These tests aimed to depict the advancements and limitations of PVs over an extended time in a simulated setting. Since the light environments were known to influence these PVs, they were effectively investigated in this study. Hence, this study provided useful insights into the performance of PVs under various environmental situations, which can inform future research and development efforts in the field.

## 2.0 METHODOLOGY

### 2.1 Design Structure of Greenhouse Chamber

Monocrystalline (9 V, 3W), polycrystalline, and amorphous PVs were purchased from SolarPowerItems, China. Initially, the PVs were placed in a chamber to facilitate various ambient temperature values in simulated environments. The main box (greenhouse) was utilised in the chamber, which was designed to conduct the simulation of different ambient temperatures. Additionally, the PVs

were mounted on the greenhouse chamber. Subsequently, five high-powered light-emitting diodes (LEDs, specifications = 1W, 120 Lm/W, 6000 K) were purchased and placed inside the greenhouse to serve as the loads for the PVs. The five LEDs were also connected in parallel with a 3 V supply. A thermoelectric Peltier module (12 V, 10 A) was applied to simulate the cold and hot weather. The simulated weather conditions were performed by cooling and heating the Peltier module's sides. All the weather simulation components were placed inside the greenhouse chamber to simulate the ambient temperature, as illustrated in Figure 1.

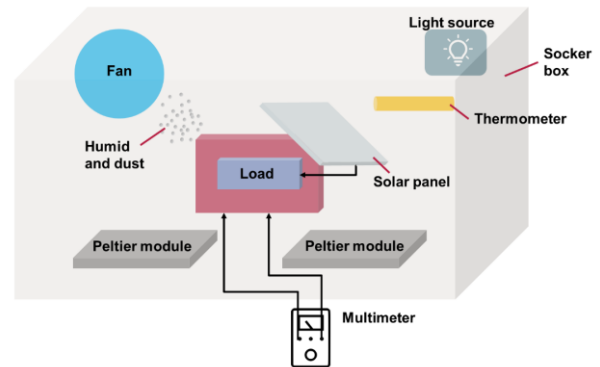


**Figure 1** Diagram representing the greenhouse chamber main design and system layout

### 2.2 Measurement of PV Performances in Simulated Environments

In the chamber design, the heater, cooler, fan, and light source wire connections were connected within the box's exterior to avoid interruption during the measurement process. Moreover, the multimeter probes were attached to the load and placed within the box's exterior to obtain accurate readings. The thermometer was also located near the PV to obtain the ambient temperature values. Five LEDs were seated inside on the top side of the greenhouse model to verify if the installed PV was functioning properly. The temperature was obtained at one-hour intervals to ensure that the solar was under the effect of the current temperature.

During the experiment, eight hours were allocated for each PV test. Weather simulation tests were performed before the experiment to avoid overheating and damage. Subsequently, the operating times to reach the desired temperatures (hot and cold) were noted. The results of the  $V_{oc}$  and  $I_{sc}$  were measured and recorded for each temperature test. Hence, the output power was calculated from the obtained values. PV modules were also installed in arid, dust-free locations, with regular cleansing and maintenance to improve PV performance.

### 2.3 Peltier Module of the Greenhouse Chamber

A typical thermoelectric module containing an array of doped bismuth telluride semiconductor pellets was connected electrically in series but thermally in parallel. Therefore, the chamber would have one cold surface and an opposite hot surface in Figure 2. Initially, the heating system was designed where a large bulk heatsink was placed on the hot surface of the Peltier. Subsequently, a small fan was mounted on top of the bulk heatsink to dissipate the heat once the heatsink became hot. Moreover, for the cold ambient temperature simulation, a central processing unit (CPU) heatsink cooler was mounted on the hot surface of the Peltier, where the heatsink did not heat up. Simultaneously, a small heatsink was mounted at the cold surface to absorb the coldness produced by the Peltier. A small fan was mounted on the small heatsink to dissipate the cold air. Finally, the prototype was placed in an enclosed room with a running air-conditioner at the lowest temperature as support.

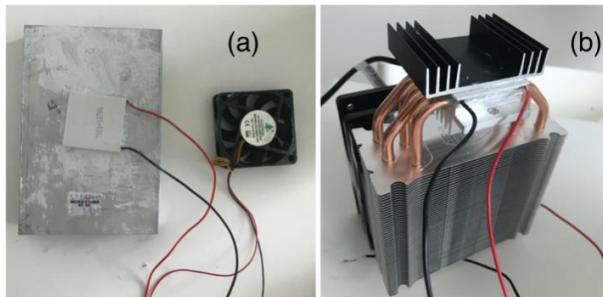


**Figure 2** Photographs of the Peltier setup for heating and cooling systems. (a) Peltier setup for the heating system with a heat dissipation fan. (b) Peltier setup for cooling system on a CPU heatsink and a small concentrating heatsink to extract the freezing characteristics

### 3.0 RESULTS AND DISCUSSION

Three main conditions were simulated using the built prototype, which produced the weather simulation of hot, cold, and room temperatures. The testing condition for each type of simulated weather was demonstrated under direct sunlight to verify the impact of the solar irradiance. Therefore, the obtained results were focused on the influence of the operating hours, temperature, and solar irradiance on different PVs. Initially, the simulation tests were investigated in a simulated sequence; hot → room → cold. After each ordeal, each PV rested for around 16 hours before conducting the next test.

The temperatures achieved within the simulation box were mainly fixed among all three solar types. The temperatures for the hot and cold conditions were approximately 40 to 42 °C and 18 to 21 °C, respectively. For the room temperature conditions, the temperature was estimated to be approximately 26 to 28 °C. All the tests were performed for 8 hours, from 8.00 pm to 4.00 am (GMT +8). This period was selected to avoid any sunlight interference, and the

PVs functioned based on artificial lighting. The experiment was repeated under direct sunlight testing. The chosen period was from 8.00 am to 4.00 pm (GMT +8) to obtain proper solar irradiance variations throughout the day.

### 3.1 PV Performance under Different Operating Hours

Initially, the influence of various operating hours on PV performance was measured across all devices (monocrystalline, polycrystalline, and amorphous). Generally, the PV performance was represented by the measurement curves in terms of  $V_{pv}$ ,  $I_{pv}$ , and power ( $P_{pv}$ ). Figure 3 depicts the variation of  $V_{pv}$ ,  $I_{pv}$ , and  $P_{pv}$  with the corresponding different temperatures (hot, room, and cold). Overall, the PV performance degraded for all PVs. The degradation process was probably due to the stress applied to the PVs throughout the operating hours. Moreover, the PV performance degradation process observed from the graphs was a reversible loss, which was reversed by rest.

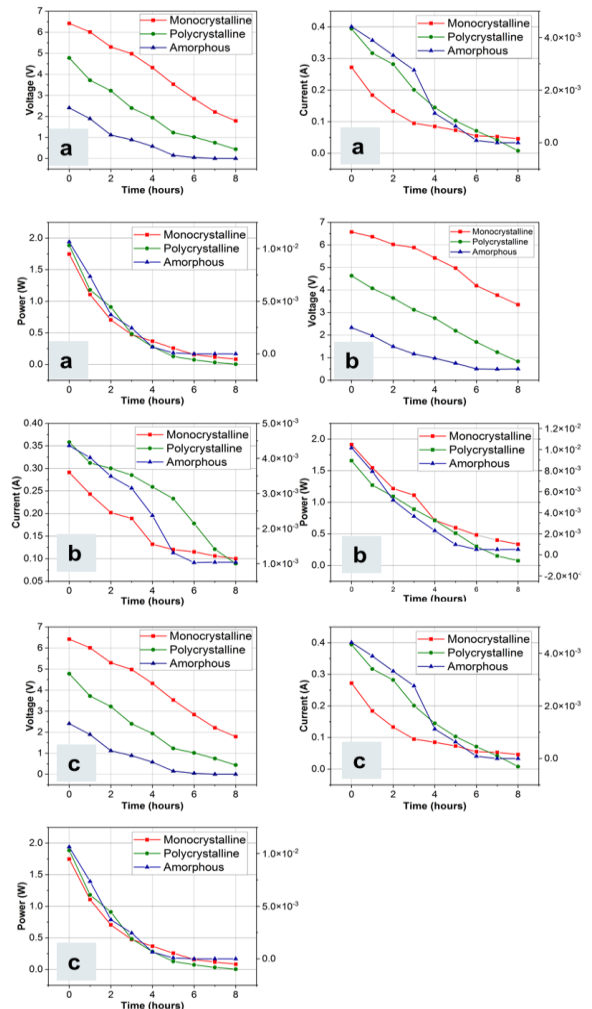


**Figure 3** The variation of  $V_{pv}$ ,  $I_{pv}$ , and  $P_{pv}$  throughout the operating hours in (a) hot weather simulation, (b) room temperature simulation, and (c) cold weather simulation. In the  $I_{pv}$  and  $P_{pv}$  graphs, the left side of the y-scale indicates monocrystalline and polycrystalline PV values, whereas the right side of the y-scale indicates amorphous PV values

Generally, the  $I_{pv}$  and  $P_{pv}$  graphs for all PVs in hot (40–42 °C) and room temperatures (26–28 °C) demonstrated exponential decay processes. Nevertheless, monocrystalline PV described a slower decay in cold temperatures (18–21 °C) than in other PVs. Thus, monocrystalline PV was more suitable in cold weather than polycrystalline and amorphous PVs. This decaying process was proposed due to the PVs increasing the  $P_{pv}$  loss throughout the operating hours.

According to the charge carriers trapping phenomenon, the PV performance decrease occurred in the surface layers of the PVs [24]. Therefore, the charge carriers trapping process reduced the electron-hole ( $e-h^+$ ) recombination pairs used to generate enough electrical signals. At higher temperatures, the band gap of semiconductor materials narrowed, generating more charge carriers. This process also increased the probability of charge carrier recombination, and multiple studies observed this effect [25,26]. Regarding the phenomenon of charge carrier entrapment, the ( $e-h^+$ ) recombination pairs required to generate sufficient electrical signals decreased, resulting in decreased PV performance. This phenomenon predominantly occurred in the surface layers of PV cells. During operation, more charge carriers became trapped in different energy gap states, reducing PV performance. Conversely, the trapped minority charge carriers retained their original condition after stopping the PV measurement. Hence, the PVs were weakened temporarily, and the process was reversed. It was also worth noting that once the next test was initiated, the PV ratings returned to their original values.

The linear degradation processes were portrayed based on the  $V_{pv}$  values for all PVs. Nonetheless, these losses were mainly bearable by all the PVs. At higher temperatures, the impact of these losses was more severe, and with time, the PV performance dropped further. Thus, several effects were causing the reduction in PV performance. Additionally, the operating hours indicated how much the PVs could sustain and withstand the reversible conditions. The reversible losses were considered temperature variations throughout the operating hours, which caused energy losses to the PV panels.

After the study tests ended, the charge carriers returned to their original state and were active in their respective layers. Furthermore, more  $P$  loss to the PV performance was introduced with longer operating hours. The long operating hours were considered a factor for the degradation since it allowed different effects on the PVs during the study tests [27]. Eventually, the charge carriers' trapping process still occurred if the operating hours were stretched along with temperatures, which the PVs recovered from afterwards.

The monocrystalline PV was illustrated to produce the least reduction in PV performance throughout the operating hours. Hence, the monocrystalline PV

acquired higher sustainability toward the degradation process than polycrystalline and amorphous PVs. The higher sustainability was due to the crystal structure of the monocrystalline PV and fabrication method, which provided a higher efficiency [28]. Furthermore, the trapping of carriers occurred in every type of PV tested [24]. On the contrary, the charge carrier trappings in the monocrystalline PV produced a weaker influence than the polycrystalline and amorphous PVs. The more invalid result was also probably due to the high crystal structure quality and the uniformity of the layers in monocrystalline PV. Consequently, due to its effective structural engineering, monocrystalline PV remained a better option for operating hours than polycrystalline and amorphous PVs.

### 3.2 PV Performance under Different Temperatures

In this study, the influence of temperature is visualised in Figure 4 for monocrystalline, polycrystalline, and amorphous PVs. Generally, all curves decreased, with the simulated cold environment (26–28 °C) displaying the best PV performance. On the contrary, PV performance reduction was highest during the simulated hot environment (40–42 °C). The reversible degradation was depicted as the main influence of this behaviour. The surrounding daily temperature and weather conditions affected the reversible degradation of the system. Hence, the PVs possessed a lower performance in the hot environment. Once the state was removed again, the PVs regained their performance.

Based on the operating temperature variation in Figure 4, the movement of the ( $e-h^+$ ) pairs leads to a variation in the PV performance [29]. The finding indicated that the direction of the electron-hole pairs was highly affected at a higher temperature, which led to a significant drop in the PV performance. In addition, the operating temperature also contributed to the performance reduction due to the charge carriers trapped. Thus, the operating temperature even demonstrated a harsher impact on the charge carriers. The effect was caused by the temperature exciting the charge carriers to move around the PV structures.

At higher temperatures, the movement of charge carriers increased, possibly changing the energy states. Through this process, the charge carriers easily get trapped [30]. Furthermore, the lattice parameter changed at elevated temperatures, and the charged carriers were trapped at higher temperatures [31]. All the charge-trapping effects mostly occurred at the top surface layers, which recovered once the PV rested after the study test. Hence, the resting process aided the recovery process when the minority carriers provided less stress inflicted upon them. The PV returned to its original state, and most carriers were active in the next recombination process. Also, the PV performance loss was demonstrated by the PVs originating from the combination of continuous testing time and

varying operating temperatures. The loss occurred in all PVs during solar energy harvesting and the charge carrier's recombination processes. Moreover, the loss process was accelerated when the increasing temperature contributes more to the charge carriers trapped by providing more energy.

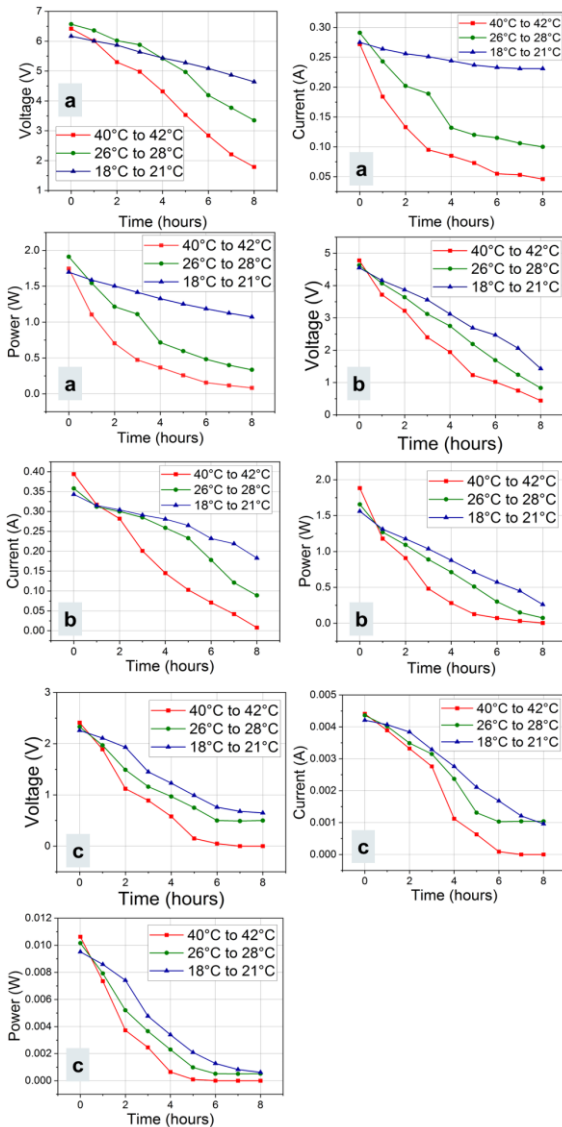


**Figure 4** The influence of surrounding temperatures (40–42, 26–28, and 18–21 °C) on (a) monocrystalline, (b) polycrystalline, and (c) amorphous PVs

Comparing the PVs, the monocrystalline PV produced the least performance reduction among other PV types regarding power rating. Additionally, the polycrystalline PV established a lower performance reduction than the amorphous PV in general. Nevertheless, the variation of the starting points of the PVs was not very critical. Although higher temperatures caused an increase of charge carriers trapped, the monocrystalline structure did not reveal layer defects that trapped more of these carriers. Therefore, the trapped charged carriers in the monocrystalline PV were less than in polycrystalline and amorphous PVs. Based on the

amorphous structure of amorphous PV, the PV acquired more significant charge carrier trapping. When the intrinsic layers exceeded the collection width, the output power density was saturated at a maximum value where the PV was limited in performance [32]. The absorbed power from the optical beam was solidly proportional to the thickness of the PV structure, which affected the carrier's mobility.

### 3.3 PV Performance under Direct Sunlight

The peaks of solar irradiance and temperatures were usually obtained from 11.00 am to 2.00 pm (GMT+8) [33]. In the investigation study (see Figure 5), the  $V_{pv}$  peaked at almost 11.00 am for monocrystalline and polycrystalline PVs. Subsequently, the performance of the monocrystalline PV decreased after 1.00 pm (peak solar irradiance time). A similar output was observed for polycrystalline PV, except it did not withstand the temperature effect even though the peak solar irradiance was achieved. Initially, the amorphous PV received enough solar irradiance, which then deteriorated with time regardless of the solar irradiance. Hence, the temperature demonstrated a higher impact on the amorphous PV.

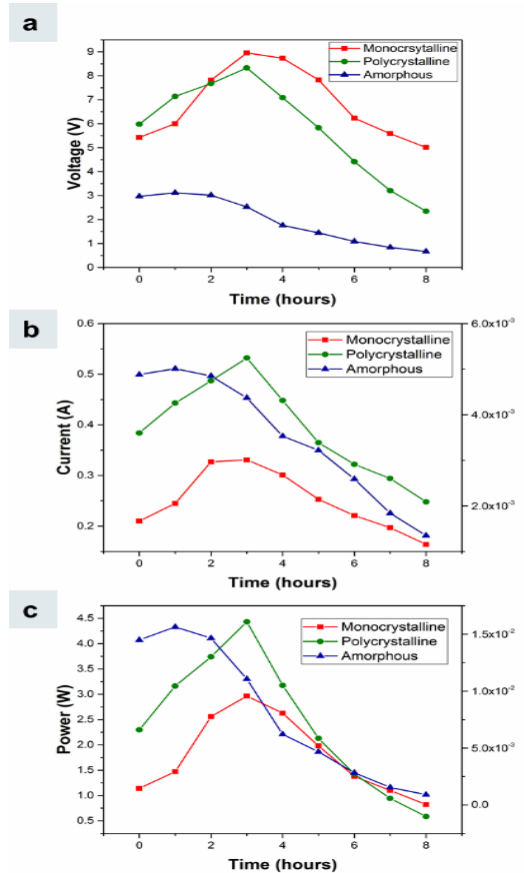


**Figure 5** The PV performance results in terms of (a)  $V_{pv}$ , (b)  $I_{pv}$ , and (c)  $P_{pv}$  for different solar PVs under direct sunlight (33–37°C) in Malaysia. In the  $I_{pv}$  and  $P_{pv}$  graphs, the left side indicates monocrystalline and polycrystalline PV values, whereas the right side of the y-scale indicates the amorphous PV values

The observations revealed that the PVs were more sensitive to the peak of the ambient temperature rather than the solar irradiance. Moreover, the  $I_{pv}$  graph described a similar concept as  $V_{pv}$ , where the monocrystalline PV seemed to withstand the temperature effect during the irradiance peak. The polycrystalline PV also peaked at 11.00 am but dropped as the temperature increased, greatly influencing the PV performance. Meanwhile, amorphous PV did not follow the solar irradiance trend. Additionally, the amorphous PV could not withstand much when the temperature increased. Lastly, the P graph also illustrated a similar behaviour, where the monocrystalline PV's performance reduction was less than that of the polycrystalline and amorphous PVs. Therefore, solar irradiance produced an impact on the PV performance curve.

The trend of increasing to a peak level before decreasing was due to less irradiance spread at the end of the test day. The solar irradiance had driven the PV performance curve to depict a variety of sunlight distribution across the PVs. Nevertheless, solar irradiance was not the leading influence for the later part of the curves' characteristics. The temperature effect provided a decent amount of impact on the PV performance curves by exhibiting the PV performance reduction even during the irradiance peak. Similarly, the test under the direct sun introduced charge carrier trapping. When the temperature peaked with the solar irradiance, the PV performance dropped due to charge carriers trapped by the temperature's effect. The temperature produced the charge carriers to be excited and to move randomly within the structure, which got trapped in a gap state. Thus, the trapped charge carriers no longer contributed to the recombination process.

Referring to the monocrystalline PV curves, the structure of the monocrystalline PV was slightly affected by the trapping of charge carriers during the peak of both solar irradiance and temperature. Moreover, the polycrystalline PV curves also revealed the impact of charge carriers' trapping. In contrast, the effect was more severe than the monocrystalline PV due to crystal structure and quality. Finally, the worst impact occurred in amorphous PV curves where the charge carrier trapping occurred almost from the beginning of the test. Thus, this observation indicated that the uniformity of the crystal in amorphous was low, and there were more carriers trapped, which led to low PV performance [34].

### 3.4 Performance Comparison between Various PVs

The reduction percentage was calculated to determine which PV type performed better along the whole measurements to compare different solar PVs. All the calculated percentages are tabulated in Table 1. Based on the results, the bar chart is plotted in Figure 6. Considering the PV performance, the monocrystalline PV produced the least performance reduction percentages among the other types. The

lowest PV performance reduction percentage for the monocrystalline PV was during the simulated cold test (see Figure 6a), with only a 16% performance reduction in the  $I_{pv}$  value. Nevertheless, the highest performance reduction percentage for the monocrystalline PV was observed at the simulated hot test (see Figure 6c), in which the P reduction reached 95%. Additionally, polycrystalline PV acquired more advantages over amorphous PV.

**Table 1** Summary of the reduction performance percentages ( $V_{pv}$ ,  $I_{pv}$ , and  $P_{pv}$ ) of different PV panels under different simulated weather and real environmental conditions

Simulated weather conditions	Parameters (Reduction performance percentages)	Types of PV		
		Monocrystalline	Polycrystalline	Amorphous
Cold temperature (18°C to 21 °C)	$V_{pv}$ (%)	25	69	71
	$I_{pv}$ (%)	16	65	77
	$P_{pv}$ (%)	37	83	93
Room temperature (26°C to 28 °C)	$V_{pv}$ (%)	49	82	79
	$I_{pv}$ (%)	66	75	76
	$P_{pv}$ (%)	82	96	95
Hot temperature (40°C to 42 °C)	$V_{pv}$ (%)	72	91	95
	$I_{pv}$ (%)	83	98	90
	$P_{pv}$ (%)	95	99	99
Direct sunlight (33°C to 37 °C)	$V_{pv}$ (%)	44	73	79
	$I_{pv}$ (%)	50	51	73
	$P_{pv}$ (%)	72	87	94

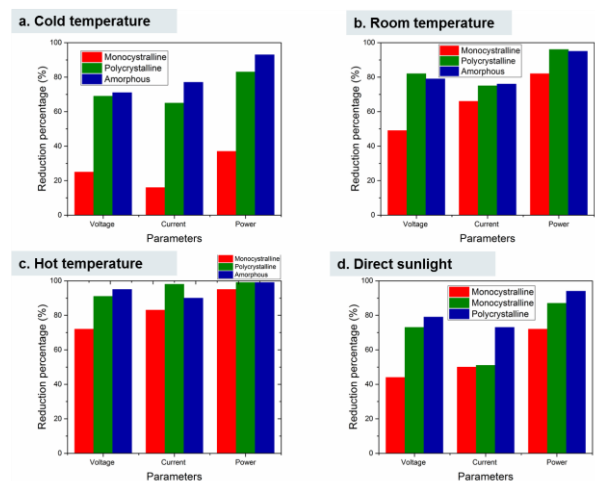


**Figure 6** Graphs indicating PV performance reduction percentage ( $V_{pv}$ ,  $I_{pv}$ , and  $P_{pv}$ ) of monocrystalline, polycrystalline, and amorphous PVs in simulated (a) cold weather, (b) room temperature, (c) hot weather, and (d) under direct sunlight

Although amorphous PV displayed a lower performance reduction percentage than the polycrystalline PV in the simulated room temperature test (see Figure 6b), the polycrystalline PV demonstrated the lowest performance reduction percentage (51%) in the simulated direct sunlight testing (see Figure 6d). Furthermore, the polycrystalline PV observed high-performance

reduction percentages overall, while the highest performance reduction percentage was achieved at the simulated hot temperature test with 99% of power reduction. Lastly, the amorphous PV acquired the most performance reduction percentages. All the power reduction percentages for the amorphous PV were above 90% for all tests, which revealed its disadvantage.

Based on the results, the percentages indicated that the monocrystalline PV performed much better than other PVs. The higher PV performance was due to the crystal formation and the fabrication procedures of the monocrystalline PVs. Moreover, the monocrystalline PV structure possessed sleeker aesthetics and higher electron flow generation [35]. Nevertheless, there was a noticeable performance reduction for all these PV types. The performance reductions were due to many reasons, such as solar irradiance, temperature, minor crystal defects, and other reversible losses like the temporary charge carriers trapping process. The effects on the PV's performance were depicted particularly for the amorphous PV during the simulated hot weather testing.

A large reduction in performance was observed for amorphous PV, which highlighted that the panel had much more stress on the structure layers causing more charge carriers to trap. There was a noticeable difference between the performance reduction percentages compared to the hot ambient temperature simulation and the direct sunlight testing. The temperature variation between these two tests was slightly different, demonstrating that solar irradiance provided better performance than LED powering the PVs. Hence, the positive effect of solar irradiance was concluded through the lower performance reduction percentage in the simulated direct sun test than in the simulated hot test. Nonetheless, the ambient temperature produced an impact under the direct sun that did not allow the performance curve to exactly follow the solar irradiance curve [36,37]. Despite that, the solar irradiance curve provided a better performance as the temperature effect still influenced it under the hot sun.

#### 4.0 CONCLUSION

This study successfully investigated the performance of different solar technologies under various ambient temperatures. Generally, all solar PVs (monocrystalline, polycrystalline, amorphous) degraded throughout operating hours. The monocrystalline PV performed better than polycrystalline silicon PV, while the amorphous silicon PV was inferior under this investigation. The performance degradation of all solar PVs was ascribed to the charge carriers' trapping in different energy gap states. Additional operating hours resulted in additional carriers' trapping and further

performance reduction. Moreover, the solar tech performance degraded the most at around 40 to 42 °C compared to the simulated room (26–28 °C) and cold temperatures (18–21 °C). All three solar PVs were tested under direct sunlight (33–37 °C), and the results demonstrated that the solar irradiance and temperature under direct sunlight influenced the PV performance. With the help of this research, the impact of ambient temperature could serve as an impetus for additional PV investigations in created simulated environments.

#### Conflicts of Interest

The author(s) declare(s) that there is no conflict of interest regarding the publication of this paper.

#### Acknowledgement

This work was partly supported by the Telekom Malaysia Research and Development (TM R&D) under TM R&D Research Fund (Grant No: RDTC/231080, Project ID: MMUE/230009)). The authors would like also to acknowledge Multimedia University (MMU, Malaysia).

#### References

- [1] A. Zekry. 2020. A Road Map for Transformation from Conventional to Photovoltaic Energy Generation and Its Challenges. *J. King Saud Univ. - Eng. Sci.* 32(7): 407-410. Doi: 10.1016/j.jksues.2020.09.009.
- [2] J. M. Kephart, A. Kindvall, D. Williams, D. Kuciauskas, P. Dippo, A. Munshi, W. S. Sampath. 2018. Sputter-Deposited Oxides for Interface Passivation of CdTe Photovoltaics, *IEEE J. Photovoltaics*, 8(2): 587-593. Doi: 10.1109/JPHOTOV.2017.2787021.
- [3] G. S. Thirunavukkarasu, M. Seyedmahmoudian, J. Chandran, A. Stajceviski, M. Subramanian, R. Marnadu, S. Alfaify, M. Shkir. 2021. Optimisation of Monocrystalline Silicon Solar Cell Devices Using PC1D Simulation. *Energies*, 14(16): 4986. Doi: 10.3390/en14164986.
- [4] R. Sagar, A. Rao. 2021. Nanoscale TiO<sub>2</sub> and Ta<sub>2</sub>O<sub>5</sub> as Efficient Antireflection Coatings on Commercial Monocrystalline Silicon Solar Cell. *J. Alloys Compd.* 862: 158464. Doi: 10.1016/j.jallcom.2020.158464.
- [5] D. M. Fébba, R. M. Rubinger, A. F. Oliveira, E. C. Bortoni, 2018. Impacts of Temperature and Irradiance on Polycrystalline Silicon Solar Cells Parameters. *Sol. Energy*, 174: 628-639. Doi: 10.1016/j.solener.2018.09.051.
- [6] S. Garud, C. T. Trinh, D. Abou-Ras, B. Stannowski, R. Schlatmann, B. Rech, D. Amkreutz, 2020. Toward High Solar Cell Efficiency with Low Material Usage: 15% Efficiency with 14 μm Polycrystalline Silicon on Glass. *Sol. RRL*, 4(6): 2000058. Doi: 10.1002/solr.202000058.
- [7] H. Park, Y. Lee, S. J. Park, S. Bae, S. Kim, D. Oh, J. Park, Y. Kim, H. Guim, Y. Kang, H.-S. Lee, D. Kim, J. Yi. 2019. Tunnel Oxide Passivating Electron Contacts for High-efficiency n-type Silicon Solar Cells with Amorphous Silicon Passivating Hole Contacts. *Prog. Photovoltaics Res. Appl.* 27(12): 1104-. Doi: 10.1002/pip.3190.
- [8] Y. Hao, W. Yang, L. Zhang, R. Jiang, E. Mijangos, Y. Saygili, L. Hammarström, A. Hagfeldt, G. Boschloo. 2016. A Small Electron Donor in Cobalt Complex Electrolyte Significantly Improves Efficiency in Dye-sensitised Solar Cells. *Nat.*

- Commun.* 7(1): 13934. Doi: 10.1038/ncomms13934.
- [9] D. Rachmat, R. Syarifah, I. Paramudita, N. Fadhilah, M. H. Haekal, R. A. Wahyuono, R. Hidayat, R. Zakaria, V. Suendo, D. D. Risanti. 2021. Au-doped Mesoporous SiO<sub>2</sub> Scattering Layer Enhances Light Harvesting in Quasi Solid-state Dye-sensitized Solar Cells. *J. King Saud Univ. - Eng. Sci.* Doi: 10.1016/j.jksues.2021.07.007.
- [10] M. Nakamura, K. Yamaguchi, Y. Kimoto, Y. Yasaki, T. Kato, H. Sugimoto. 2019. Cd-Free Cu(In,Ga)(Se,S)<sub>2</sub> Thin-Film Solar Cell With Record Efficiency of 23.35%. *IEEE J. Photovoltaics.* 9(6): 1863-1867. Doi: 10.1109/JPHOTOV.2019.2937218.
- [11] W. Septina, C. P. Muzzillo, C. L. Perkins, A. C. Giovanelli, T. West, K. K. Ohtaki, H. A. Ishii, J. P. Bradley, K. Zhu, N. Gaillard. 2021. In situ Al<sub>2</sub>O<sub>3</sub> Incorporation Enhances the Efficiency of CuIn(S,Se)<sub>2</sub> Solar Cells Prepared from Molecular-ink Solutions. *J. Mater. Chem. A.* 9(16): 10419-10426. Doi: 10.1039/D1TA00768H.
- [12] G. T. S. How, N. A. Talik, B. K. Yap, H. Nakajima, S. Tunmee, B. T. Goh. 2019. Multiple Resistive Switching Behaviours of CH<sub>3</sub> NH<sub>3</sub> PbI<sub>3</sub> Perovskite Film with Different Metal Electrodes. *Appl. Surf. Sci.* 473(October 2018): 194-202. Doi: 10.1016/j.apsusc.2018.12.124.
- [13] M. A. Green. 2009. The Path to 25% Silicon Solar Cell Efficiency: History of Silicon Cell Evolution. *Prog. Photovoltaics Res. Appl.* 17(3): 183-189. Doi: 10.1002/pip.892.
- [14] T. Saga. 2010. Advances in Crystalline Silicon Solar Cell Technology for Industrial Mass Production. *NPG Asia Mater.* 2(3): 96-102. Doi: 10.1038/asiamat.2010.82.
- [15] K. L. Chopra, P. D. Paulson, V. Dutta. 2004. Thin-film Solar Cells: An Overview. *Prog. Photovoltaics Res. Appl.* 12(23): 69-92. Doi: 10.1002/pip.541.
- [16] M. Chaichan, H. A. Kazem. 2016. Experimental Analysis of Solar Intensity on Photovoltaic in Hot and Humid Weather Conditions. *Int. J. Sci. Eng. Res.* 7: 91-96.
- [17] K. Akhmad, A. Kitamura, F. Yamamoto, H. Okamoto, H. Takakura, Y. Hamakawa. 1997. Outdoor Performance of Amorphous Silicon and Polycrystalline Silicon PV Modules. *Sol. Energy Mater. Sol. Cells.* 46(3): 209-218. Doi: 10.1016/S0927-0248(97)00003-2.
- [18] N. Amin, C. W. Lung, K. Sopian. 2009. A Practical Field Study of Various Solar Cells on Their Performance in Malaysia. *Renew. Energy.* 34(8): 1939-1946. Doi: 10.1016/j.renene.2008.12.005.
- [19] A. Q. Malik, S. J. B. H. Damit. 2003. Outdoor Testing of Single Crystal Silicon Solar Cells. *Renew. Energy.* 28(9): 1433-1445. Doi: 10.1016/S0960-1481(02)00255-0.
- [20] W. Tress, K. Domanski, B. Carlsen, A. Agarwalla, E. A. Alharbi, M. Graetzel, A. Hagfeldt. 2019. Performance of Perovskite Solar Cells under Simulated Temperature-illumination Real-world Operating Conditions. *Nat. Energy.* 4(7): 568-574. Doi: 10.1038/s41560-019-0400-8.
- [21] C. Xiao, X. Yu, D. Yang, D. Que. 2014. Impact of Solar Irradiance Intensity and Temperature on the Performance of Compensated Crystalline Silicon Solar Cells. *Sol. Energy Mater. Sol. Cells.* 128: 427-434 Doi: 10.1016/j.solmat.2014.06.018.
- [22] A. Almuwailhi, O. Zeitoun. 2021. Investigating the Cooling of Solar Photovoltaic Modules under the Conditions of Riyadh. *J. King Saud Univ. - Eng. Sci.* Doi: 10.1016/j.jksues.2021.03.007.
- [23] J. Adeeb, A. Farhan, A. Al-Salaymeh. 2019. Temperature Effect on Performance of Different Solar Cell Technologies. *J. Ecol. Eng.* 20(5).
- [24] G. Juška, K. Genevičius, N. Nekrašas, G. Sliaužys. 2010. Charge Carrier Transport, Recombination, and Trapping in Organic Solar Cells Studied by Double Injection Technique. *IEEE J. Sel. Top. Quantum Electron.* 16(6): 1764-1769. Doi: 10.1109/JSTQE.2010.2041752.
- [25] A. M. Smith, S. Nie. 2010. Semiconductor Nanocrystals: Structure, Properties, and Band Gap Engineering. *Acc. Chem. Res.* 43(2): 190-200.
- [26] X. Deng, X. Liao, S. Han, H. Povolny, P. Agarwal. 2000. Amorphous Silicon and Silicon Germanium Materials for High-efficiency Triple-junction Solar Cells. *Sol. Energy Mater. Sol. Cells.* 62(1-2): 89-95.
- [27] H. Hashigami, Y. Itakura, T. Saitoh. 2003. Effect of Illumination Conditions on Czochralski-grown Silicon Solar Cell Degradation. *J. Appl. Phys.* 93(7): 4240-4245. Doi: 10.1063/1.1559430.
- [28] N. S. Baghel, N. Chander. 2022. Performance Comparison of Mono and Polycrystalline Silicon Solar Photovoltaic Modules under Tropical Wet and Dry Climatic Conditions in East-central India. *Clean Energy.* 6(1): 165-177. Doi: 10.1093/ce/zkac001.
- [29] T. Leijtens, G. E. Eperon, A. J. Barker, G. Grancini, W. Zhang, J. M. Ball, A. R. S. Kandada, H. J. Snaith, A. Petrozza. 2016. Carrier Trapping and Recombination: the Role of Defect Physics in Enhancing the Open Circuit Voltage of Metal Halide Perovskite Solar Cells. *Energy Environ. Sci.* 9(11): 3472-3481. Doi: 10.1039/C6EE01729K.
- [30] F. Feldmann, G. Nogay, P. Löper, D. L. Young, B. G. Lee, P. Stradins, M. Hermle, S. W. Glunz. 2018. Charge Carrier Transport Mechanisms of Passivating Contacts Studied by Temperature-dependent J-V Measurements. *Sol. Energy Mater. Sol. Cells.* 178: 15-19. Doi: 10.1016/j.solmat.2018.01.008.
- [31] E. Schiff. 2003. Low-mobility Solar Cells: A Device Physics Primer with Application to Amorphous Silicon. *Sol. Energy Mater. Sol. Cells.* 78(1-4): 567-595. Doi: 10.1016/S0927-0248(02)00452-X.
- [32] M. Filipič, Z. C. Holman, F. Smole, S. De Wolf, C. Ballif, M. Topič. 2013. Analysis of Lateral Transport through the Inversion Layer in Amorphous Silicon/crystalline silicon Heterojunction Solar Cells. *J. Appl. Phys.* 114(7): 074504. Doi: 10.1063/1.4818709.
- [33] N. Aoun, K. Bouchouicha, R. Chenni. 2016. Performance Evaluation of a Monocrystalline Photovoltaic Module Under Different Weather and Sky Conditions. *Int. J. Renew. Energy Res.* 7: 292-297.
- [34] B. Wang, G. M. Biesold, M. Zhang, Z. Lin. 2021. Amorphous Inorganic Semiconductors for the Development of Solar Cell, Photoelectrocatalytic and Photocatalytic Applications. *Chem. Soc. Rev.* 50(12): 6914-6949. Doi: 10.1039/D0CS01134G.
- [35] H. Biermann, M. Strehler, H. Mughrabi. 1996. High-temperature Measurements of Lattice Parameters and Internal Stresses of a Creep-deformed monocrystalline Nickel-base Superalloy. *Metall. Mater. Trans. A.* 27(4): 1003-1014. Doi: 10.1007/BF02649768.
- [36] F. Bayrak, H. F. Oztop, F. Selimefendigil. 2019. Effects of Different Fin Parameters on Temperature and Efficiency for Cooling of Photovoltaic Panels under Natural Convection. *Sol. Energy.* 188: 484-494. Doi: 10.1016/j.solener.2019.06.036.
- [37] S. K. Yadav, U. Bajpai. 2018. Performance Evaluation of a Rooftop Solar Photovoltaic Power Plant in Northern India. *Energy Sustain. Dev.* 43: 130-138z. Doi: 10.1016/j.esd.2018.01.006.